Integrative Organismal Biology

A Journal of the Society for Integrative and Comparative Biology

academic.oup.com/iob

OXFORD UNIVERSITY PRESS

Integrative Organismal Biology

Integrative Organismal Biology, obae020
https://doi.org/10.1093/iob/obae020

A Journal of the Society for Integrative and Comparative Biology

ARTICLE

Morphology and Mechanics of the Fin Whale Esophagus: The Key to Fast Processing of Large Food Volumes by Rorquals

K.N. Gil [*,1] A.W. Vogl[†,1] and R.E. Shadwick[*,1,2]

[*]Department of Zoology, University of British Columbia, Vancouver, BC V6T 1Z4, Canada; [†]Life Sciences Institute and Department of Cellular and Physiological Sciences, University of British Columbia, Vancouver, BC V6T 1Z3, Canada

[1]These authors contributed equally to this work.
[2]E-mail: shadwick@zoology.ubc.ca

Synopsis Lunge feeding rorqual whales feed by engulfing a volume of prey laden water that can be as large as their own body. Multiple feeding lunges occur during a single foraging dive and the time between each lunge can be as short as 30 s (Goldbogen et al. 2013). During this short inter-lunge time, water is filtered out through baleen to concentrate prey in the oral cavity, and then the prey is swallowed prior to initiating the next lunge. Prey density in the ocean varies greatly, and despite the potential of swallowing a massive volume of concentrated prey as a slurry, the esophagus of rorqual whales has been anecdotally described as unexpectedly narrow with a limited capacity to expand. How rorquals swallow large quantities of food down a narrow esophagus during a limited inter-lunge time remains unknown. Here, we show that the small diameter muscular esophagus in the fin whale is optimized to transport a slurry of food to the stomach. A thick wall of striated muscle occurs at the pharyngeal end of the esophagus which, together with the muscular wall of the pharynx, may generate a pressure head for transporting the food down the esophagus to the stomach as a continuous stream rather than separating the food into individual boluses swallowed separately. This simple model is consistent with estimates of prey density and stomach capacity. Rorquals may be the only animals that capture a volume of food too large to swallow as a single intact bolus without oral processing, so the adaptations of the esophagus are imperative for transporting these large volumes of concentrated food to the stomach during a time-limited dive involving multiple lunges.

Synopsis (Icelandic translation) Fæðuöflun reyðarhvala (ein af 4 ættum skíðishvala) felur í sér að gleypa sjó sem í er blönduð sú bráð sem sóst er eftir hverju sinni, en magn sjávarins að þyngd getur jafnast á við þyngd þess hvals sem veiðir. Margar gleypingar geta átt sér stað í hverri veiði köfun og tími milli gleypinga getur verið stuttur eða allt niður í 30 sekúndur (Goldbogen et al. 2013). Á þessum stutta milli-gleypingar tíma er sjór síaður út milli skíðanna og þeirri bráð sem eftir situr í munnholinu er kyngt, áður en til næstu gleypingar kemur. ðéttni bráðar í hafinu er mjög breytileg og þrátt fyrir getu reyðarhvala að kyngja miklu magni af samþjappaðri og ómeðhöndlaðri bráð, þá hefur vélinda þeirra verið lýst sem óvenjulega þröngu og lítt eftirgefanlegu líffæri. Hvernig reyðarhvalir fara að því að kyngja svo miklu magni fæðu niður um þröngt og stíft vélinda, á stuttum milli-gleypingar tíma, er óþekkt. Í þessari grein sýnum við fram á hvernig þetta þrönga vöðvaklædda vélinda skíðishvala er byggt, til að hámarka flutning á ómeltri fæðu frá munnholi í maga. Á mótum vélinda og koks er þykkur veggur þverráka vöðva sem er samfléttaður þverráka vöðvum koks en þessir kröftugu vöðvar geta þrýst stöðugum straumi fæðu úr koki, um vélinda og niður í maga, frekar en að um kyngingu einstakra skammta sé að ræða. ðetta einfalda líkan er í samræmi við mat á þéttleika bráðar og getu magans að taka við. Reyðarhvalir eru væntanlega einu dýrin sem gleypa svo mikið magn fæðu, sem ekki er hægt að kyngja í einstaka skömmtum og því er aðlögun á vélinda nauðsynleg til að flytja (dæla stöðugt) þetta mikla magn af ómeltri fæðu niður í magann á meðan á, oft stuttum, veiðiköfunum stendur sem einnig geta haft með að gera margar gleypingar.

Introduction

Rorqual whales, the lunge feeding baleen whales, are the largest filter feeding animals. Bulk feeding on small aggregating prey enables access to large amounts of energy at lower trophic levels, which is required for rorquals to maintain large body sizes (Goldbogen and Madsen 2018; Goldbogen et al. 2019). Lunge feeding has been described as the largest biomechanical event on the planet (Brodie 1993) and involves a rorqual accelerating toward a patch of prey and opening its mouth to engulf

a volume of prey-laden water that can be larger than its own body volume (Goldbogen et al. 2007, 2010). This process is repeated successively during a foraging dive, with each lunge averaging 16 s and the interval between lunges averaging 30 s in fin whales (Goldbogen et al. 2006, 2007). During the inter-lunge interval, the engulfed water is filtered out through the baleen plates to concentrate the prey in the oral cavity while the oral plug remains in position, followed by swallowing of the prey when the oral plug is retracted (Gil et al. 2022)—a process that must be completed before the whale can open its mouth for the next lunge. Therefore, the inter-lunge interval must consist of both filtration and swallowing. Since swallowing remains unstudied in rorquals, we are unaware of its time course, but it must be a significant factor in determining lunge timing and frequency. The dimensions and actions of the esophagus dictate how rapidly food travels to the stomach.

Generally in mammals, the esophagus is a hollow muscular tube responsible for transporting food from the pharynx to the stomach. At rest, the esophagus is dorsoventrally flattened, but it opens and stretches to accommodate food. The esophageal wall is composed of four tissue layers: mucosa, submucosa, muscularis propria, and adventitia, from the lumen outwards (Gregersen 2003; Oezcelik and DeMeester 2011; Young et al. 2014; Pawlina and Ross 2016). The mucosa is composed of epithelium, the lamina propria (connective tissue) and the muscularis mucosae (smooth muscle fibers), and it possesses longitudinal folds along the inner lumen surface to allow expansion during food transport. The submucosa is composed of blood vessels, lymphatics, and connective and nerve tissues. The muscularis propria is a muscular bilayer, with an inner layer of circular muscle fibers and an outer layer of longitudinal muscle fibers. The adventitia is the outermost layer of the esophagus and is a connective tissue layer that wraps around the muscularis propria and connects the esophagus to surrounding structures.

The muscularis propria is responsible for sequential contractions that create waves of peristalsis to transport a bolus along the esophagus to the stomach and dictates the time it takes to swallow food. The muscularis propria, in addition to its differently oriented muscle fibers (inner circular and outer longitudinal) is composed of striated muscle in the cervico-thoracic esophagus and smooth muscle in the abdominal esophagus (caudal to the diaphragm), with the transition zone commonly occurring in the thoracic region. The proportion of muscle type along the esophagus impacts the rate of peristalsis, where esophagi with higher striated muscle content have faster peristalsis (Sukon 2002).

Anecdotal references suggest that the rorqual esophagus is remarkably small; for example, in a blue whale that can be up to 29 m long the esophagus is "unable to stretch more than 10 inches" (Scales and Smith 2010) in width. Personal observations from necropsies show the esophagus of an ~21-m long adult fin whale has an esophagus only ~10 cm in outer width, with a very thick internal wall. Plotting outer esophageal width (from literature and necropsies) against body mass for terrestrial mammals and cetaceans, it is clear the baleen whale esophagus is dramatically smaller than expected from isometric scaling, with the effect being even more pronounced when esophageal lumen width is considered instead (Fig. 1). With such a narrow esophagus in an animal so big, it is unknown how large volumes of food are transported to the stomach during the short inter-lunge period after filtering.

Mathematical models of fin whale buccal cavity and ventral groove blubber (VGB) inflation have produced estimates of the amount of water engulfed per lunge (Goldbogen et al. 2006, 2007; Potvin et al. 2009); however, the amount of prey captured in a lunge varies depending on prey density, patch size, and distribution in the environment (Goldbogen et al. 2015). Additionally, measurements of krill density span across orders of magnitude depending on the time of sampling and the method used to sample (Goldbogen et al. 2011). Krill densities that rorquals may encounter and feed on vary, but are estimated to be as high as 154 kg/m^3 from studies unrelated to whale presence (Nicol et al. 1987); however, such high values are likely overestimates. Feeding frequency in rorquals increases with prey density to maximize energy intake (Goldbogen et al. 2015; Hazen et al. 2015); thus, the potential exists for rorquals to engulf large quantities of prey should they encounter them, as it is most energetically advantageous.

Food transport along the esophagus by peristalsis is generally similar across mammals; however, the distinct morphology of the rorqual esophagus with its astonishingly small lumen and thick wall, and the fact that these whales are bulk feeders suggest the esophagus is not just a scaled-up version of an average mammalian esophagus. Here, we use dissection of post-mortem animals, histological analysis of samples, and mechanical tests of isolated organs to explore how the fin whale esophagus is optimized to allow transport of a large quantity of food from the pharynx to the stomach in a short period of time.

Methods

Animals and tissue samples

Fin whale specimens were collected postmortem in the summers of 2015 and 2018 as part of the commercial

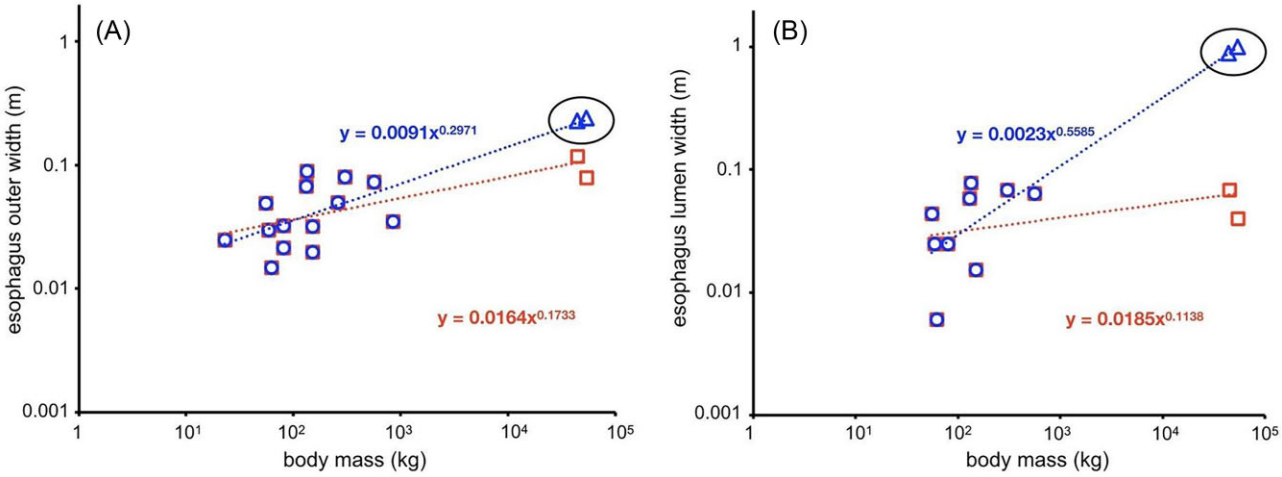

Fig. 1 Scaling plots of terrestrial mammal, odontocete, and mysticete esophagi outer width vs. body mass (A), and lumen width vs. body mass (B) plotted on log axes. The far right points on both graphs are for mysticetes. The red trendlines and equations are for terrestrial mammals, odontocetes, and mysticetes plotted together. The blue trendlines and equations are for terrestrial mammals and odontocetes, with the equation from those mammals applied to mysticete body masses to plot where mysticete data would fall if they scaled in the same way, indicated by triangle markers and circled in black. For a fin whale (50,000 kg), actual esophageal outer width is 0.118 m and predicted is 0.226 m (A); actual esophageal lumen width is 0.069 m and predicted is 0.884 m (B). For a bowhead whale (55,000 kg), actual esophageal outer width is 0.08 m and predicted is 0.241 m (A); actual esophageal lumen width is 0.04 m and predicted is 0.993 m (B). Esophageal widths were collected from literature or measured in this study. In most cases, an average body mass used here was identified in the literature. Animals used in both outer diameter and lumen diameter plots include human, South Asian river dolphin14, bowhead whale15, fin whale, harbor porpoise, Pacific white-sided dolphin*, common dolphin, Dall's porpoise, Risso's dolphin, Beluga*, and false killer whale* (personal observations). Additionally, the outer diameter plot included llama12, sheep12, cow12, spinner dolphin16*, and bottlenose dolphin16*. * = measured specimen body mass; no star indicates estimated body mass based on size.

catch operation at Hvalfjörður, Iceland. Whales were dissected and mechanical tests were performed within 36 h of death. All animals examined were adults. A total of 17 esophagi were examined with 5 of those contributing to the mechanical data and 4 contributing to histology. Tissue samples were imported to Canada under Convention on International Trade in Endangered Species of Wild Fauna and Flora (CITES) permits.

A Pacific white-sided dolphin was collected at a necropsy of animals stranded and recovered along the coast of British Columbia, Canada, by Fisheries and Oceans Canada. Histological samples were collected within 48 hours of the necropsy that was performed shortly after the animal's death.

Gross anatomy

In fin whales, the viscera of the whale from the pharynx to anus was removed in a single piece. The esophagus was revealed by cutting through thick fascia in the midline dorsally between the lungs. The esophagus was then removed whole—rostrally from the posterior end of the pharynx at the level of the inferior pharyngeal constrictor (cricopharyngeus), and caudally from directly thoracic to the diaphragm. Length was measured. Photos were taken throughout the revealing and removal process. A single esophagus was sliced down its length longitudinally to examine changes in muscle type and thickness in the wall.

In the Pacific white-sided dolphin, the viscera from tongue to stomach was removed. The esophagus was removed from the surrounding tissue. Photos were taken of the esophagus throughout the removal and during subsequent experiments.

Inflation tests

The esophagi of five fin whales were inflated with water. Water was run through the esophagus prior to inflation to ensure the esophagus was clean and empty. A pipe fitting attached to a water hose was inserted into the caudal end of the esophagus and secured with a metal hose clamp around the esophagus. The rostral end of the esophagus was plugged with a pipe fitting attached to a simple tube manometer, and a metal hose clamp was tightened around the esophagus. The esophagus was filled with water to condition the tissue and was drained until the manometer had a "0" pressure reading. The length of the esophagus was measured. The esophagus was then inflated to an estimated "max inflation/pressure", which corresponded with no further visible width increase. Photos were taken before

inflation and at max pressure. Max pressure and the inflated length were recorded. After inflation, the water in the esophagus was drained into a bucket down to the 0 pressure mark and weighed for a volume estimate. The remaining water to empty the esophagus was drained and weighed to determine total esophageal volume.

Outer dimensional changes and the percentage of expansion along the esophagus were measured from photos using Fiji (Schindelin et al. 2012). Landmarks on the esophagus ensured the same location was consistently measured for width. Changes in wall thickness before inflation and at max inflation were calculated. The inner radius of the inflated esophagus, r_i, for each segment (anterior, middle, and posterior) was calculated with

$$r_i = \sqrt{r_o^2 - \left(R_o^2 - R_i^2\right) L/l}, \tag{1}$$

assuming constant wall volume (Lillie et al. 2013), where r_o is the inflated outer radius, R_o is the unloaded outer radius, R_i is the unloaded inner radius, L is the unloaded length, and l is the inflated length. Circumferential wall stress, σ_w, in the inflated esophagus was calculated with r_i for each segment using the Law of Laplace formula:

$$\sigma_w = \frac{P_i r_i}{h_i}, \tag{2}$$

where P_i is the inflated esophagus pressure and h_i is the inflated wall thickness. Wall stress relative to esophageal position during inflation was calculated for each segment of the esophagus.

Esophageal volume was determined from the calculated inner radius by applying the inner radius of each segment to one-third of the total esophagus length and summing the values. The calculated esophageal volume was compared with the measured esophageal volume from the inflation to confirm the accuracy of the inner radius calculation.

To determine if the esophageal muscle at max inflation would be able to overcome the inflation pressure to produce a peristaltic contraction, we calculated the stress, or pressure, that the circular muscle could produce at full inflation/expansion for each segment tested, using the calculated wall thickness and inner radius at maximum inflation. We assumed that each wall layer (mucosa/submucosa, circular muscle, and longitudinal muscle) decreased in thickness equally, so divided the wall thickness by 3 to account for just the circular muscle layer. A reasonable average specific muscle tension (i.e., stress or force per unit area) for vertebrate striated muscle is 200 kPa (Rospars and Meyer-Vernet 2016). This same value was used for the entire esophagus, even the smooth muscle region, which means the values produced for smooth muscle may be an overestimate of the force production that the smooth muscle is actually capable of. The formula used to calculate the pressure the muscle could generate, P, was

$$P = \sigma_m \, h \, / \, r, \tag{3}$$

where σ_m is specific muscle tension, h is wall thickness, and r is radius.

Uniaxial stretch tests

Uniaxial stretch tests were performed on the esophagi of five fin whales. Segments of esophagus ~20 cm long were cut from the anterior, middle, and posterior regions, with an attempt to cut the segments from the same approximate location in each esophagus. One piece at a time was tested. The section of esophagus was placed on a wet table to reduce friction and two 2.5 cm wide bars were placed through the lumen of the esophagus. One of the bars was fastened to a metal cable with eye bolts and cable clamps at either end of the bar, with the esophagus between these attachment points. The metal cable was hooked around a force transducer connected to DataQ hardware (Dataq DA Convert DI-205; Dataq Instruments Inc. Akron, OH, USA; sampling rate 10 Hz) synced with WinDaq software (version 1.37 Dataq Instruments Inc.) to record force measurements. The other bar was manually pulled away steadily from the bar affixed to the force transducer, opening and stretching the esophageal lumen. A video camera was fixed above the set-up to record the extensibility of the esophagus. The force recording and video were synced up by tapping the force transducer and providing an auditory cue at the same time. A video camera beside the set-up provided a side view of the lumen being stretched. Each esophageal section was stretched 3 times, allowing for conditioning of the tissue with the final stretch for analysis. During the last stretch, the bar was pulled until no further stretch was obtainable ("max" stretch was reached). All esophagus pieces were photographed to measure dimensions. Video and photo data were analyzed in Fiji (Schindelin et al. 2012). The stretched distance was measured at one frame per second up to the maximum distance, which was the final measurement. The mechanical length of the tissue was calculated as

$$length = \pi r_m + 2r_{ib} + D, \tag{4}$$

where D is the measured stretch distance between bars, r_m is the midwall radius, and r_{ib} is the bar radius, to account for the tissue wrapped around the bars that

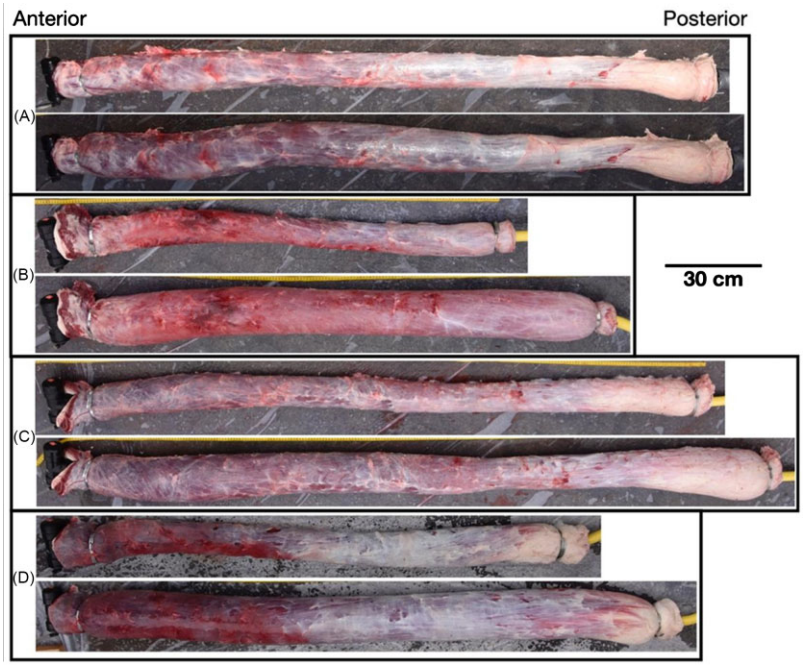

Fig. 2 Uninflated (top of panels) and inflated (bottom of panels) esophagi of four fin whales. (A)—esophagus 2, (B)—esophagus 3, (C)—esophagus 4, and (D)—esophagus 5. Posterior (stomach) is to the left and anterior (pharynx) to the right. The difference in overall tissue color (white posteriorly and red anteriorly) demonstrates a difference in muscle type, where whiter tissue is smooth muscle and redder tissue is striated muscle. However, not all colors are indicative of differences in muscle type; the esophagus is covered with a layer of adventitia that obscures some of the tissue colors but displays a darker red in the anterior region as it connects the esophagus to other tissues and organs. The bottom left of (D) shows interdigitation of the two muscle types along the outer layer. Not all esophagi inflated equally. In (A), there is a restriction in the posterior region, and in (C), there is a restriction between middle and posterior regions. Scale bar–30 cm.

is also being stretched (Lillie et al. 1994). Midwall in this case denotes the outer edge of the circular muscle layer, calculated as two-thirds of the total wall thickness. The longitudinal muscle layer does not restrict expansion of the esophagus; therefore, only the circular muscle was considered. Stress vs. stretch ratio graphs were produced from these data. To combine and compare all the fin whale data, linear interpolation was used on the stress and stretch data from each segment to determine the stress at 0.05 stretch ratio intervals and new graphs were plotted. Inflated wall stress and the corresponding stretch ratio, calculated from width expansion in inflation photos, was plotted on the stress vs. stretch ratio graphs to compare the two mechanical tests. The dimensions of all esophagus segments used in uniaxial tests were measured from photos using Fiji (Schindelin et al. 2012) and compiled to determine trends in morphology along the length of the esophagus.

Histology

Thoracic esophagus tissue was sampled from the anterior, middle, and posterior regions of two fin whale esophagi and processed for histology. These sampling locations corresponded with the segments tested in the uniaxial stretch tests. The Pacific white-sided dolphin esophagus tissue was sampled from anterior and posterior thoracic regions. All samples were fixed in 10% neutral buffered formalin, and then processed by Wax-it Histology Services Inc. (University of British Columbia), following standard techniques. Samples were sliced at 5 μm thickness and stained with Verhoeff–Van Gieson stain to display elastin in black, collagen in pink, and muscle in yellow/beige. Slides were scanned using an Aperio AT2 whole slide scanner (Leica) and the digitized images used for analysis. The relative proportions of muscle in each region were confirmed using a conventional light microscope.

Results

Gross and microscopic anatomy

Whales ranged from 15.55 to 19.42 m in length with an esophagus length range from 1.29 to 1.90 m, measured from the caudal end of the pharynx to the thoracic side of the diaphragm (Fig. 2). The esophagus was a flattened hollow cylinder and was oval in cross section at both anterior (cranial) and posterior (caudal) ends, and occasionally more circular in the middle (Fig. 3). The average outer esophageal width across all

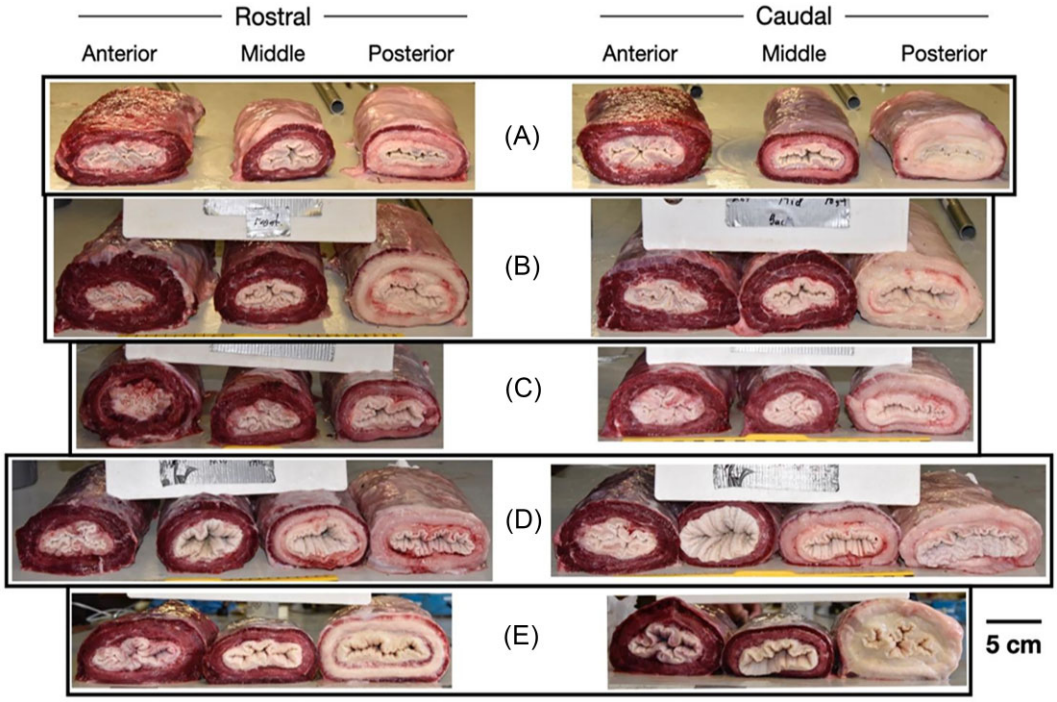

Fig. 3 Esophageal segments from five fin whales used in uniaxial stretches. (A)—esophagus 1, (B)—esophagus 2, (C)—esophagus 3, (D)—esophagus 4, and (E)—esophagus 5. Esophageal segments arranged from left to right are anterior, middle, and posterior. In (D), the second segment from the right was an additional sample; the far right segment is the posterior segment. Left column—rostral faces of segments, right column—caudal faces of segments. The esophageal lumen is wavy and folded to varying degrees. The anterior segments show deep folds in addition to the wavy epithelium lining. Middle segments are generally similar in appearance to the anterior segments with more deep folds. Posterior segments show fewer deep folds but consistent epithelial waviness. In (D), the posterior segment shows rugae indicative of a transition to forestomach rather than being strictly esophageal tissue. The tissues directly surrounding the inner lumen are the mucosa and the submucosa; the boundary between them is difficult to distinguish from gross anatomy. The mucosa appears to contain a lot of adipose tissue, especially in some of the posterior segments, for example in panel (E). Surrounding the mucosa and submucosa is the muscular bilayer. The two muscle layers are easily distinguished in most segments. Deep red colored muscle is striated muscle (example indicated by the black arrow) and pink/white colored muscle is smooth muscle (example indicated by the white arrow). There are varying amounts of striated muscle extending into the posterior region, especially in the outer longitudinal muscle layer. There is variation in the shape of the esophageal segments. Scale bar–5 cm.

fin whales and all segments of esophagus was 11.8 cm across (largest axis of the oval); however, width varied along the length of the esophagus with the smallest width in the middle region, corresponding with the change in shape from oval to circular (Table 1). Lumen width increased along the length of the esophagus to its widest at the posterior end, with a corresponding decrease in wall thickness. Thickness of the individual muscle layers decreased overall and the mucosa/submucosa layer was thickest in the middle. The epithelium lining the lumen was quite wavy with deep folds; the degree of folding was less pronounced in the posterior segments (Fig. 3). The anterior, approximately three-fourths of the esophageal muscle, was thick, stiff and deep red in color. The posterior one-fourth of the esophagus qualitatively was more compliant than the first three-fourths and ranged from pink to white in color (Figs. 2 and 3). Cross sections along the esophagus confirmed a muscular transition from completely striated muscle in both muscle layers at the anterior end to a combination of striated and smooth at the posterior end. The transition of muscle type began around two-thirds of the way along the esophagus and was a gradual transition—there was no distinct point where a switch in muscle type occurred. Additionally, the two muscle layers didn't transition at the same location; the inner circular layer was often solely smooth muscle in the posterior-most esophagus, but the outer longitudinal layer often had a combination of striated and smooth muscle well into the posterior-most esophagus (Fig. 3). The longitudinally sliced esophagus confirmed these muscular transitions from anterior to posterior.

Histological analysis confirmed this transition of muscle type through the esophagus and displayed additional morphological changes along esophagus

Table 1 Average esophagus dimensions and morphological trends ($n = 5$); means with standard deviation (±s.d.)

Measurement	Anterior	Middle	Posterior	Change along length
Outer width (m)	0.127	0.106	0.122	Narrows at middle
(±s.d.)	±0.012	±0.008	±0.008	
Lumen width (m)	0.063	0.064	0.078	Increase
(±s.d.)	±0.013	±0.009	±0.012	
Wall thickness (m)	0.032	0.030	0.027	Decrease
(±s.d.)	±0.005	±0.012	±0.004	
Longitudinal muscle thickness (m)	0.010	0.007	0.006	Decrease
(±s.d.)	±0.003	±0.01	±0.0001	
Circular muscle thickness (m)	0.010	0.008	0.008	Decrease then holds
(±s.d.)	±0.001	±0.002	±0.001	
Mucosa & submucosa thickness (m)	0.012	0.015	0.013	Thickest at middle
(±s.d.)	±0.003	±0.011	±0.004	
Midwall radius (m)	0.034	0.032	0.031	Decrease
(±s.d.)	±0.004	±0.008	±0.003	
Wall area (m^2)	0.014	0.012	0.012	Decrease then holds
(±s.d.)	±0.003	±0.004	±0.002	
Circular muscle area (m^2)	0.004	0.003	0.004	Smallest at middle
(±s.d.)	±0.001	±0.001	±0.0005	

(Figs. 4 and 5). The mucosa was thick in all regions sampled. In the anterior region, the lamina propria of the mucosa was characterized by a thick layer of dense collagen fibers along with a layer of diffuse adipose tissue supported by a framework of collagen (Fig. 5A). Elastin was more prevalent closer to the muscularis mucosae that was extensive and composed of a relatively thick layer of striated muscle. A few smooth muscle islands and many striated muscle islands were scattered along the innermost edge of the muscularis mucosae (Fig. 5B). The submucosa was thin and composed of dense collagen and elastin fibers, lymphatics, and blood vessels. The muscularis propria surrounding the submucosa did not always show distinct layers in the cross sections (Fig. 4A,B), but these layers were clear in the longitudinal sections (Fig. 4C). The muscularis propria of the esophagus was thicker than the other esophageal layers, forming the largest component of the esophageal wall. Both the circular and longitudinal muscle layers were about the same thickness. Within the muscle layers were many large bands of dense collagen and elastin fibers (Fig. 5C).

The middle region showed different proportions of the esophageal layers. The lamina propria collagen layer was thinner, with a thicker adipose layer extending closer toward the epithelium (Fig. 5D). The muscularis mucosae was again extensive and composed mostly of striated muscle; however, there were patches of mixed striated and smooth muscle (Fig. 5E). The islands of muscle on the lamina propria side of the muscularis mucosae were composed of smooth or striated muscle, but striated muscle islands were still more numerous. The submucosa again was thin and composed of dense collagen and elastin fibers and blood vessels. As in the anterior, the muscularis propria was the thickest portion of the esophageal wall and the two muscle layers were about the same thickness. The muscularis propria was composed mostly of striated muscle, but bands of smooth muscle were visible throughout both circular and longitudinal layers (Fig. 5F). Collagen and elastin fibers were woven throughout the muscularis propria.

The posterior region again showed a change in proportions of the esophageal layers. The lamina propria collagen layer was almost non-existent and hugged the edge of the epithelium, while the adipose layer was much thicker and extended nearly to the epithelium (Fig. 5G). Smooth muscle dominated this region, with no visible striated muscle in histological samples. The adipose layer of the lamina propria was replete with smooth muscle islands (Fig. 5H). The islands extended to the muscularis mucosae and were larger closer to the muscularis mucosae. It was not possible to tell the difference between the lamina propria layer and the muscularis mucosae. The muscle layer of the muscularis

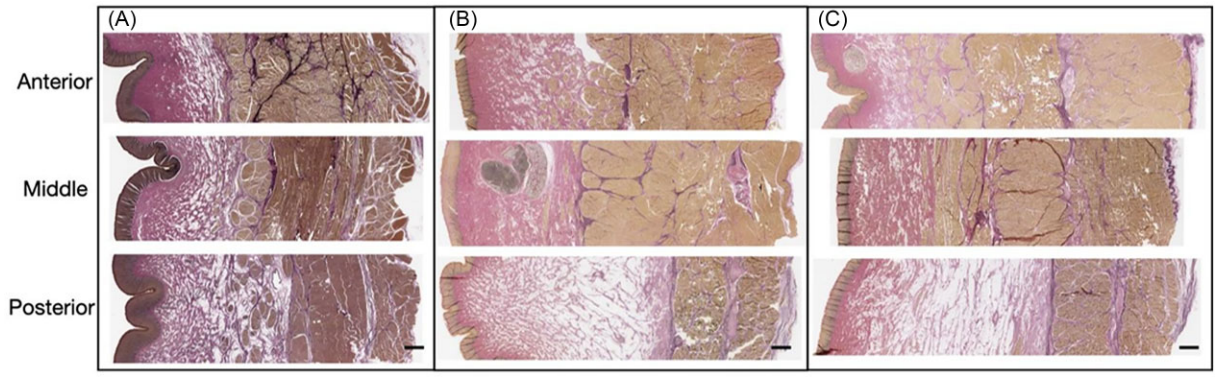

Fig. 4 Esophageal histology from two fin whales. Top of panels—anterior region, middle of panels—middle region, bottom of panels—posterior region. (A) and (B) cross sections of esophageal tissue, (C) longitudinal sections from same locations and specimen as (B). Collagen stains pink, elastin stains black, muscle stains brown/tan, most other tissues stain brown or grey, while adipose appears white (unstained). The esophageal lumen is to the left. The epithelium is visible as a brown/tan band running down the left side of all of the images. Immediately to the right of this is the lamina propria, composed of collagen, adipose, islands of muscle, and in the anterior and middle regions a distinct band of muscle. The submucosa is not large or obvious in these specimens, but exists as a small band of connective tissue (arrows) between the muscularis mucosae and the muscular bilayer of the muscularis propria. The muscularis propria consists of an inner layer of circular muscle and outer layer of longitudinal muscle. The regions of muscle (including muscularis mucosae) are most easily distinguished in the longitudinal sections (C). From anterior to posterior, there is a decrease in thickness of the collagen in the lamina propria and a corresponding increase in the thickness of adipose tissue. The anterior region of the muscularis propria is striated tissue, the middle is mostly striated tissue with scattered bands of smooth muscle, and the posterior is smooth muscle. The muscularis mucosae is more band-like in appearance in anterior and middle sections but appears as more diffuse islands in the posterior region. Specimen (B)/(C) has very little muscularis mucosae present in the posterior region. Both layers of the muscularis propria decrease in thickness posteriorly, and this change is more evident in the longitudinal muscle layer. Lymphoid nodules are visible in the middle image of panel (B) as gray ovals in the lamina propria. Scale bars—2 mm.

mucosae was less extensive than in the regions anterior to this. The submucosa was very thin. The muscularis propria was composed entirely of smooth muscle. Collagen and elastin fibers were present in the muscularis propria in thinner bundles than in anterior and middle regions, though a layer of collagen and elastin between the circular and longitudinal muscle layers appeared more distinctive but less dense than in the anterior and middle regions (Fig. 5I). The two muscle layers of the muscularis propria again had similar thicknesses.

The Pacific white-sided dolphin esophagus had similar tissue arrangements, but differing proportions and thicknesses of tissue compared to the fin whale (Fig. 6). Three major differences were noted. First, there was no diffuse adipose tissue in any region of the dolphin esophagus. Instead, the lamina propria of the mucosa was composed almost entirely of dense collagen fibers. Second, the muscularis mucosae did not have a distinct muscle layer but was composed only of islands of muscle that were comparatively less abundant than in the fin whale. Lastly, the submucosa was relatively much thicker in the dolphin compared to the fin whale.

In the anterior region of the dolphin esophagus, the muscularis mucosae was composed of sparse striated muscle islands that appeared to be localized to certain regions along the circumference of the esophagus. The submucosa was relatively thicker than in the fin whale. The muscularis propria was composed of striated muscle and both the inner circular and outer longitudinal layer were a similar thickness. Collagen and elastin fibers were woven throughout the striated muscle as in the fin whale.

The posterior region of the dolphin esophagus was similar in morphology to the anterior, the main difference being muscle type. The muscularis mucosae muscle islands were composed of smooth muscle rather than striated, and they were more abundant and more evenly distributed than in the anterior. The submucosa was thicker in the posterior region compared with anterior. The muscularis propria was composed entirely of smooth muscle. There appeared to be more collagen and especially more elastin fibers running through the muscle bilayer in the posterior region compared with the anterior region. The inner circular layer was at least double the thickness of the outer longitudinal muscle layer.

Inflation mechanics

Only four esophagi were used in comparative inflation data as the protocol differed for one esophagus.

The esophagi inflated quite easily and expanded in all directions, taking on a circular shape in cross section along the length, compared to the flattened resting state

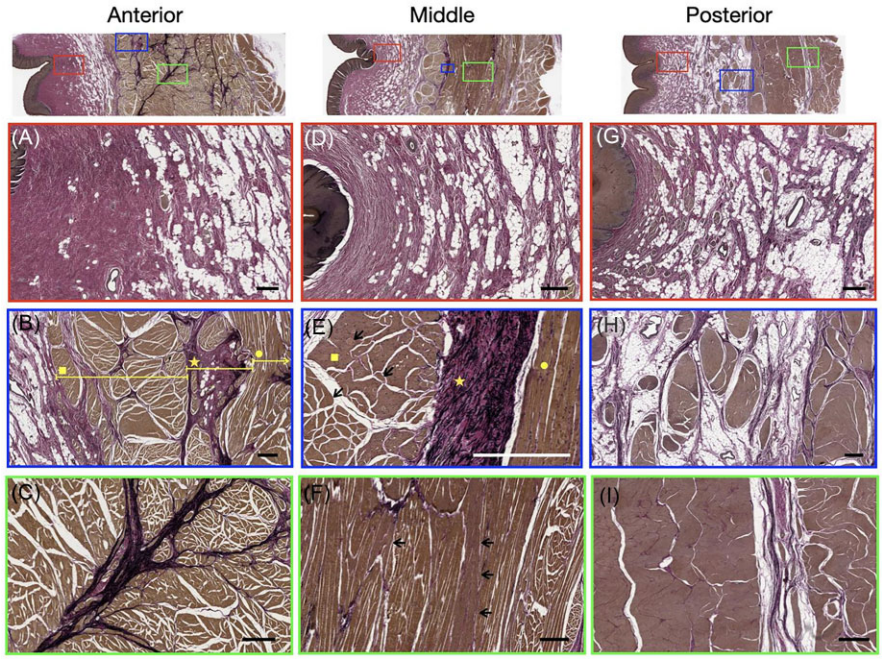

Fig. 5 Esophageal tissue at higher magnification from the anterior (ABC), middle (DEF), and posterior (GHI) regions of a fin whale esophagus. The top row of images shows the corresponding locations that the colour-coded panels display. Collagen stains pink, elastin stains black, muscle stains brown/tan, other tissues (epithelium, lymphatic) stain brown or gray, adipose appears as white (unstained). (A) The left side of the image shows a dense and thick layer of collagen, and the right side shows adipose tissue, both in the lamina propria. (B) Lamina propria is visible as the collagen and adipose tissue on the right side. The region indicated by the square is the muscularis mucosae, the star is the submucosa, and the circle is part of the circular muscle layer of the muscularis propria. (C) Dense collagen and elastin band running through striated muscle of the muscularis propria. (D) A thinner and less dense layer of collagen, but thicker layer of adipose tissue than in the anterior region. (E) The square indicates the muscularis mucosae. Though most of the muscularis mucosae is striated muscle, this image highlights part of the muscularis mucosae that has a high smooth muscle content with pockets of striated muscle indicated by the arrows. The star indicates the submucosa, which in this region is dense collagen and elastin fibers. The circle indicates the circular muscle layer of the muscularis propria. (F) A combination of striated and smooth muscle constitutes the muscularis propria. Striated muscle is dominant, and smooth muscle regions are indicated by arrows. (G) A thin layer of collagen and a diffuse extensive layer of adipose compose the lamina propria. (H) The lamina propria and muscularis mucosae are visible in this image, though the boundary between the two is not clear. Smooth muscle islands exist in the adipose layer of the lamina propria. The smooth muscle band along the right side is the muscularis mucosae. (I) The muscularis propria is composed solely of smooth muscle. A comparatively less dense band of collagen and elastin fibers define the boundary between the two muscle layers of the muscularis propria. Scale bars—500 m.

(see Fig. 2). The extracted esophagus lengths varied from 1.3 to 1.9 m. During the inflation test, esophagi were inflated until there was no more visible increase in width that resulted in inflation pressures from 6.9–8.8 kPa (Table 2). The esophagi increased in length by 6–25%, and width increase varied widely: anterior 26–34%, middle 25–70%, and posterior 6–51%. The volumes of water removed to deflate the esophagi back to 0 pressure ranged from 16 to 24 L, and the total volume to empty the esophagi varied from 18 to 27 L. The estimated esophageal luminal volumes calculated from wall thickness and lumen radius matched well with the measured esophageal luminal volumes, varying from 15 to 29 L.

Calculated wall stress in inflated esophagi increased from the anterior to the posterior end (Fig. 7). This corresponds with the change in muscle type from striated to smooth, the increase in the lumen width, and the decrease in wall thickness from anterior to posterior ends of the esophagus. The predicted pressure that the circular muscle layer can produce as a cylinder to overcome the inflation pressure was determined from the calculated muscle thickness at max inflation (Table 3). The ability for circular muscle to contract against the inflation pressure decreases posteriorly, corresponding again with the changes listed above. For all esophagi, the anterior region, on average, can overcome the inflation pressure to a greater extent than more posterior regions.

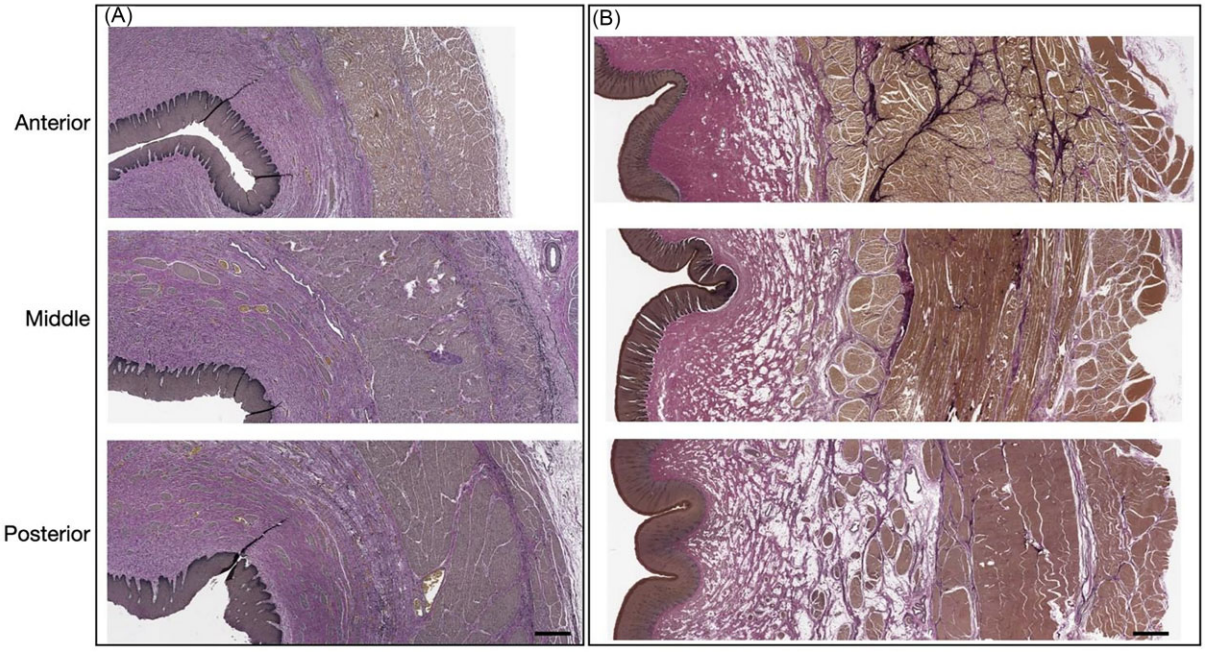

Fig. 6 Comparison of esophageal histology from a Pacific white sided dolphin (A) and fin whale (B). Side by side images do not accurately correspond with equivalent sampling locations. In (A), top image—anterior region, middle image—posterior region, bottom image—abdominal region. In (B), panels and description follow as in Figs. 4 and 5, top image—anterior region, middle image—middle region, bottom image—posterior region. Collagen stains pink, elastin stains black, muscle stains brown/tan, other tissues (epithelium, lymphatic) stain brown or gray, and adipose appears white (unstained). Both (A) and (B) demonstrate similar tissue arrangement; however, the abundances and thicknesses of the tissues and the layers varies. In the dolphin (A), the mucosa is substantial; the lamina propria is replete with collagen fibers, but adipose tissue is not present. The muscularis mucosae does not form a distinct muscle band and instead forms islands of striated muscle in the anterior region and islands of smooth muscle in the posterior and abdominal regions. The islands of muscle increase in abundance through the posterior and abdominal sections, and the boundary between lamina propria and muscularis mucosae becomes unclear; the islands of muscle penetrate the collagen layer of the lamina propria. The submucosa is relatively thicker compared to that in the fin whale (B) and increases in thickness toward the abdominal section. Elastin fibers (black) and blood vessels (blood in gold/yellow) are visible in the submucosa and increase in abundance abdominally. The muscularis propria is composed of striated muscle in the anterior region and smooth muscle in the posterior and abdominal regions. The inner circular layer and outer longitudinal layer are about the same thickness in the anterior region. There is an increase in the thickness of the circular layer and a decrease in the thickness of the longitudinal layer in both posterior and abdominal regions. Scale bars: A—500 m and B—2 mm.

Table 2 Esophageal inflation data ($n = 4$)

Esophagus	Inflation P (kPa)	Volume to 0P (L)	Total volume (L)	Length increase (%)	Anterior width increase (%)	Middle width increase (%)	Posterior width increase (%)
2	8.8	21.1	22.8	6	27	32	6
3	7.4	15.6	18.4	21	37	70	51
4	6.9	16.5	21.9	12	26	25	43
5	7.3	23.5	27.2	25	34	48	33
Average	7.6	19.2	22.6	16	31	43.8	33.3

The change in muscle type, morphology, and ability to generate force along the esophagus all indicate that the anterior region is built for and important for the force generation required for peristalsis.

Uniaxial mechanics

Segments for uniaxial stretches (shown in Fig. 3) were cut from the previously inflated esophagi. Table 4 provides the distance along the extracted esophagus that

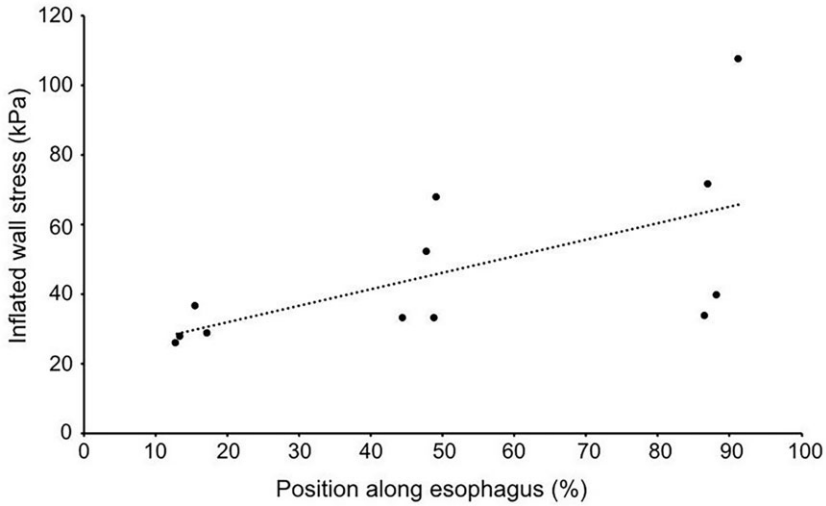

Fig. 7 Wall stress vs. position along the esophagus. Anterior is toward 0 and posterior is toward 100. Wall stress is the product of pressure and inner radius divided by wall thickness. The increase in stress toward the posterior end is the result of the decreasing wall thickness and increasing lumen diameter toward the posterior region.

Table 3 Measured inflation pressure and calculated pressure that muscle can generate as a cylinder ($n = 4$)

Esophagus	Inflation (kPa)	Calculated anterior (kPa)	Calculated middle (kPa)	Calculated posterior (kPa)
2	8.8	21.3	17.8	17.6
3	7.4	17.3	7.3	6.9
4	6.9	17.8	14.0	4.3
5	7.3	12.6	8.8	11.6
Average	7.6	17.3	12.0	10.1

Table 4 Percentage along extracted esophagus length that segments for uniaxial stretch were sampled from ($n = 5$)

Esophagus	Anterior (%)	Middle (%)	Posterior (%)
1	18	50	76
2	14	45	87
3	17	49	87
4	13	49	91
5	16	48	88

segments were cut from, to link inflation and uniaxial data and check the consistency of mechanics.

Stress vs. stretch ratio graphs showed little difference across all esophageal regions at low stresses except for three outliers (Fig. 8), indicating that regardless of differences in muscle type along the esophagus, the passive ability to restrict expansion is similar. Connective tissue, primarily collagen, controls the restriction of the esophagus rather than muscle tissue; the uniaxial stretches demonstrated the passive mechanics of the esophagus, and the increasing slope of the curves at higher stretch values shows where collagen acts to resist further expansion and prevent tissue damage. The lower stretch values, before the collagen is fully loaded, demonstrate the biologically relevant zone, and are likely representative of the stress and stretch that the esophagus will experience during bolus transport. Inflated wall stress and stretch ratio plotted on the uniaxial graphs fell in the low stress region (<100 kPa, except for one outlier) close to the corresponding uniaxial curves (Fig. 9), corroborating the biologically relevant zone. One caveat to this interpretation is that uniaxial tests on isolated segments results in higher compliance than would occur in an intact esophagus.

Outliers existed in three esophagi tested (esophagi 1, 2, and 4). The anterior region of esophagus 1 had extra outer longitudinal muscle bands along approximately half the total length of the segment (Fig. 3A). The mechanical response may also be due to rigor mortis. The posterior region of esophagus 2 showed a narrowing just cranial to the diaphragm (Fig 2A). There was limited expansion in this region in inflation tests (~6%), indicating there was some difference in this specimen that affected the mechanics and extensibility. There were no obvious morphological indications of why this region behaved differently, but again, rigor mortis was a possibility. In esophagus 4, the posterior region was sampled further caudally than the other esophagi; the lumen had rugae rather than longitudinal folds, indicative of a transition to the forestomach rather than

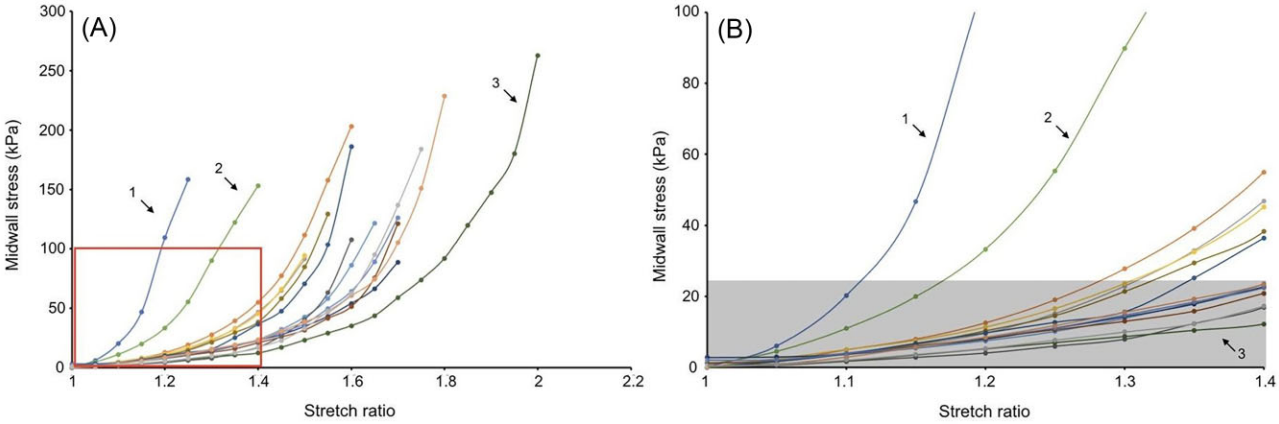

Fig. 8 Stress–stretch ratio plots of all esophageal segments tested in uniaxial stretch tests. Colors represent individual esophagus segments. (A) Complete data set of uniaxial stretches. Stresses remain low for the first half of the total stretch and gradually increase as the segments become stiffer in the latter half of the total stretch. The low stress and stretch zone is likely the biologically relevant zone, before the segments increase in stiffness as collagen restricts further expansion. The red box indicates this area, expanded in (B). (B) The biologically relevant portion of the graph, where stresses are low, is indicated by the gray box. There is little difference across all esophageal segments in this region, indicating the passive mechanics of the esophagi are all similar, despite differences in muscle or adipose content. Three outliers exist that possibly can be explained by examining the morphology of the segments. Outlier 1 (esophagus 1, anterior) had lateral muscle bands, likely extensions of pharyngeal muscle, that could have increased the stiffness of the esophagus (see Fig. 3A). Despite working with fresh tissue, this segment could also have been in rigor mortis, increasing the stiffness of the segment. Outlier 2 (esophagus 2, posterior) did not have any obvious morphological indications of why it was so stiff (see Fig. 3B). Inflation tests showed little inflation in the posterior region (Fig. 2A). Rigor mortis could have affected this segment. Outlier 3 (esophagus 4, posterior) was much less stiff than the other segments as it included a portion of the stomach (Fig. 3D).

being a strictly esophageal sample (Fig. 3D). Additionally, for esophagus 4 more than 3, segments were sampled, which limited our ability to recut the esophagus to get an esophageal sample of similar dimensions to the other segments.

Discussion

The esophagus in the fin whale is a muscular thick-walled cylinder with a small lumen, evolved to transport a slurry of food to the stomach. While the narrow or small width appearance of the esophagus seems counterintuitive based on body size and the immense mouthfuls of food they are engulfing, the morphology and mechanics of the esophagus are likely intricately linked to feeding/food type and are optimized for transporting fluid-like content. The variation in muscle type, proportion, and thickness, and the small yet extensible lumen may be keys to the function of the esophagus.

The fin whale esophagus has a variable morphology along its length, summarized in Fig. 10. The anterior region was characterized by a small lumen and thick walls composed of abundant striated muscle and collagen. These components provide the anterior esophagus with its "stiff" character, and the thick striated muscle allows the esophagus to generate large forces and pressures for peristalsis. The middle region showed some deviation from these characteristics: an increased lumen width, decreased wall thickness, similar striated muscle content, but less collagen. The posterior region also showed increased lumen width, decreased wall thickness, and decreased collagen content. Additionally, there was a large increase in adipose tissue, and a shift to smooth muscle rather than striated, giving the posterior esophagus it's more compliant structure. Based on these varying characteristics along the esophagus, including dense striated muscle content in the anterior two-thirds of the esophagus, we conclude that the anterior two-thirds of the esophagus is the main force generating and propulsive region of the structure. The muscle in this region is thick and can produce high pressures (Table 3), and because the muscle is striated, it can produce rapid peristaltic contractions (Sukon 2002). In a dog, which has almost entirely striated muscle in its esophagus, peristalsis speeds are as fast as 10 cm/s (Sukon 2002); therefore, we could assume a similar peristalsis speed, based on muscle type, in the fin whale.

As a bolus is pushed into the esophagus, the small lumen expands, and the esophageal muscles relax to accommodate the bolus. The consistency of the krill (and likely some water) being swallowed is likely an amorphous slurry—as opposed to large chunks of meat, and the esophagus wall must be able to contract down behind the bolus to push it toward the stomach. The ability for muscle to contract and decrease the lumen

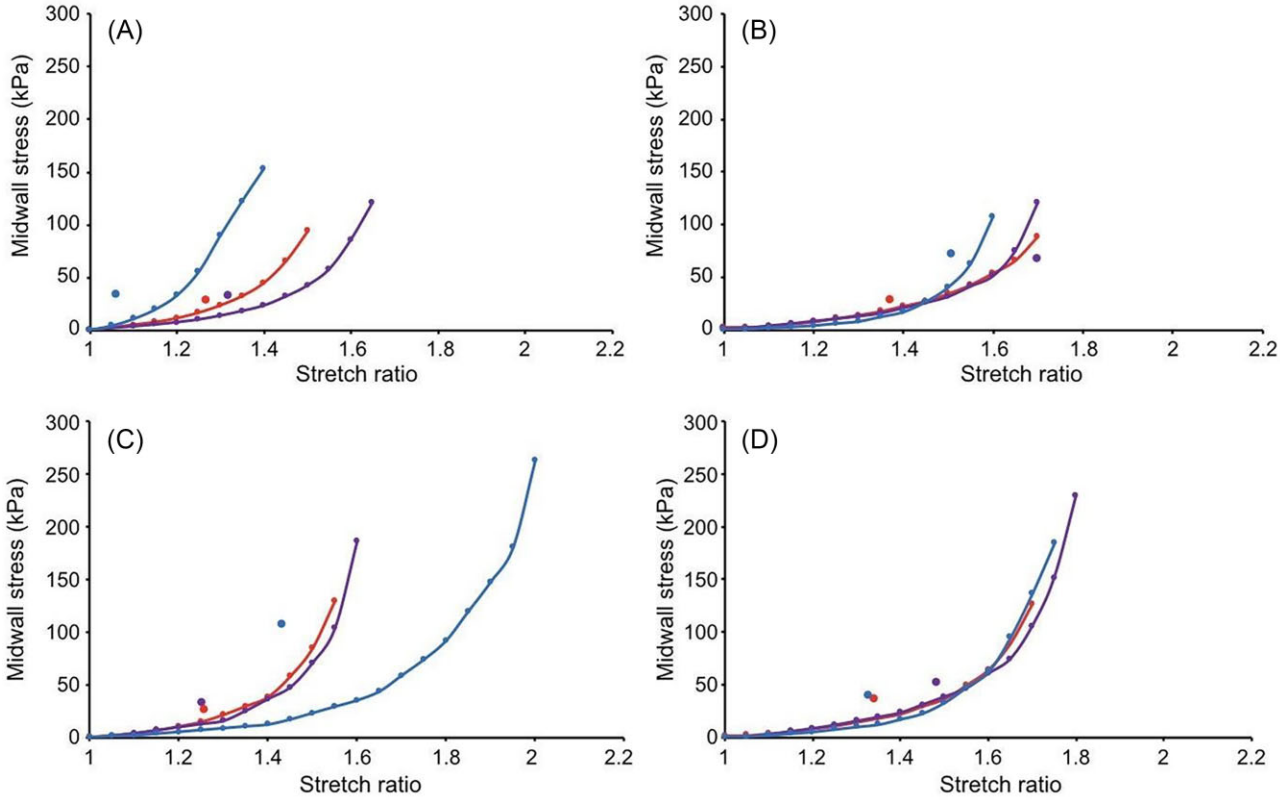

Fig. 9 Stress–stretch ratio curves with inflation data (points) for four fin whale esophagi. (A)—esophagus 2, (B)—esophagus 3, (C)—esophagus 4, and (D)—esophagus 5. Red—anterior, purple—middle, and blue—posterior. Inflation data indicated by the points on the graphs matched the uniaxial data well. Inflation stresses all fell under the 100 kPa mark (most under 50 kPa), with the exception of the posterior of esophagus 4 (C, addressed in Fig. 8). Another exception is the posterior region of esophagus 2 (A), which showed a low inflation stress and stretch (also addressed in Fig. 8). Combined inflation and uniaxial data corroborate the biologically relevant zone being the low stress zone, with the esophagi generally stretching less than 60%.

circumference behind a bolus being transported along the esophagus is limited by a muscle's ability to shorten (~25–30%). A large lumen means a bolus, especially an amorphous one, may not expand the lumen very much, and the muscle would be unlikely to contract enough to significantly decrease lumen size to push a bolus forward. Therefore, a small lumen is needed so that a fluid-like bolus can force the lumen open and the muscle can contract to decrease lumen circumference and push the bolus toward the stomach. Additionally, if the esophagus in its resting state had an enlarged and floppy lumen, then much more muscle would be needed to generate the same pressures (following Laplace; Equation 2) required for swallowing. With the morphology and mechanics of the esophagus as described above, the anterior region of the esophagus then acts as a pressure head to continually pump food down the esophagus. The thick walls and high collagen content of the esophagus enable it to resist the pressures associated with peristalsis. Additionally, in a living mammal, both the circular and longitudinal muscle layers contract during peristalsis and combined ultrasound and manometry studies show maximum pressure during peristalsis coincides with maximum wall thickness because of both muscle layers contracting simultaneously (Pehlivanov et al. 2001; Puckett et al. 2005). This means an increase in wall thickness relative to lumen width, which, according to Laplace's law (Equation 2) maintains a constant wall stress and prevents an esophageal diverticulum, the equivalent of an aneurysm, in the esophagus (Mittal et al. 2006).

Combining esophageal mechanics with krill densities from the literature and active muscle mechanics from other mammals allowed us to produce a simple model for swallowing in a fin whale. A fin whale is capable of engulfing 60–82 m^3 (average 71 m^3) in a single lunge (Goldbogen et al. 2007). To account for fin whales not always completely filling their oral cavities during a lunge (Arnold et al. 2005), we include an alternate estimate of 30 m^3 in a single lunge

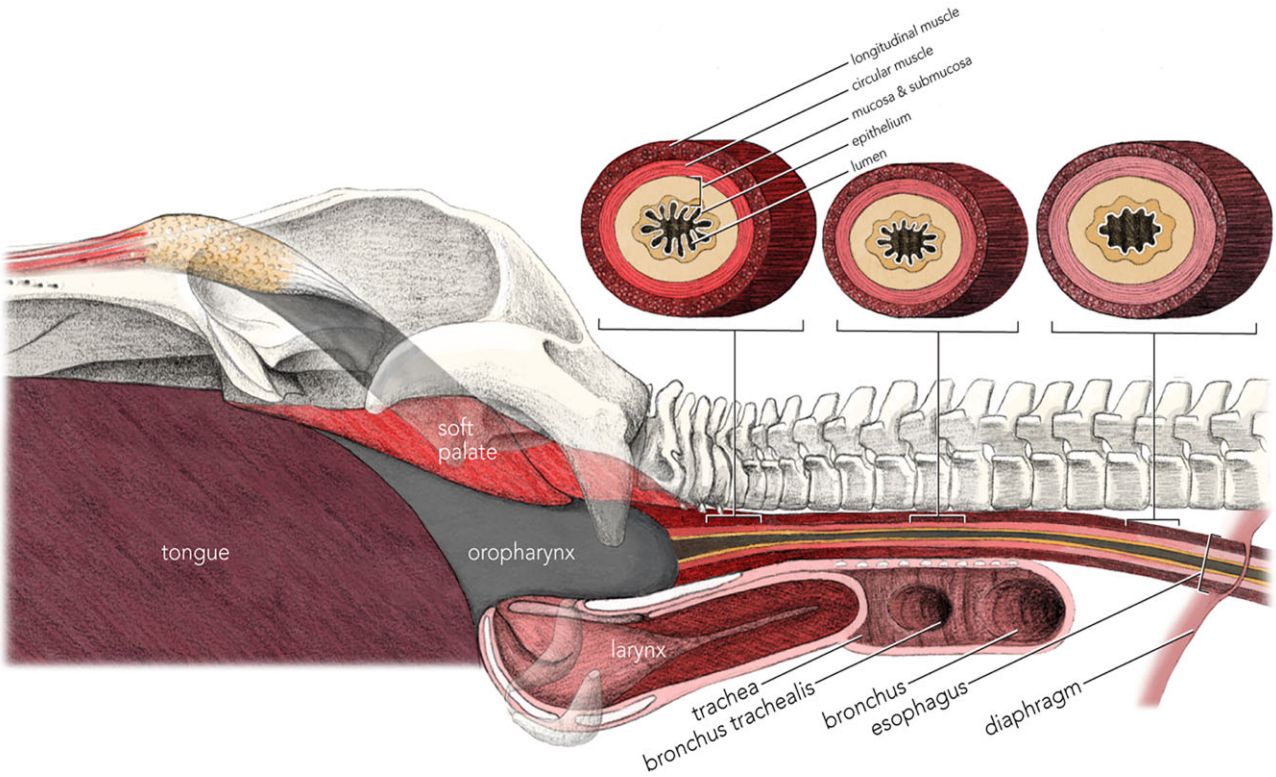

Fig. 10 General model of the structures investigated in the upper aerodigestive tract in a fin whale. The tongue fills the oral cavity and pushes food to the oropharynx. The upper airways are protected from food incursion by elevation of the soft palate and oral plug, plugging the nasopharynx. The lower airways are protected through closure of the larynx, collapse of the laryngeal sac, and movement of the larynx anteroventrally. Esophageal muscle type, relative layer thicknesses, and relative changes in lumen morphology are displayed in both the long section and cross sections of esophagus. Illustration by Alex Boersma ©2022.

(Goldbogen et al. 2006). These swallowed volumes include the krill and accompanying water. Water is filtered out through the baleen plates, but some residual volume is likely necessary to enable the swallowing process. Here, we estimate that an additional volume equivalent to 10% of the total krill volume is swallowed water—if 100 L of krill are being swallowed then 10 L of water will be swallowed with the krill, resulting in a total volume swallowed of 110 L. For a range of krill densities from the literature, we can estimate how much krill and water might be swallowed with each lunge (Tables 5, 6), with krill mass converted to volume using the specific gravity of krill as 1.025g/mL, assuming krill are isosmotic to seawater. Unfortunately, bolus size is unknown. Instead, if we assume an average esophageal capacity of 22 L, we can then determine how many swallows at maximum esophagus capacity would be required to get the mouthful to the stomach.

This reveals the first limitation in feeding frequency—transferring food from the mouth to the stomach, with limited esophagus capacity, to clear the mouth for the next lunge. Generally, in mammals, the food taken into the mouth in one bout does not exceed the capacity of the esophagus. In rorquals, however, it is likely that the food volume in the mouth from each lunge will exceed the esophageal capacity if krill density is greater than about 0.3 kg/L for a lunge volume of 71 m^3 or 0.6 kg/L for a lunge volume of 30 m^3. These estimates suggest that feeding at higher krill densities that are well within observed values could result in a "bottleneck" in food processing that limits feeding activity. If the krill captured in one lunge overfills the esophagus, then additional inter-lunge time would be needed to swallow multiple boluses to clear the mouth and/or pharynx of food in preparation for the next lunge. Even with a rapid peristalsis rate, such as 10 cm/s as in a dog (Sukon 2002), it would take 19 s for a single bolus to travel through the longest esophagus (1.9 m) examined in this study. Individual primary peristaltic contractions, the "normal" peristaltic contractions, are followed by a refractory period, which means it would take more than 19 s before the esophagus could enact another peristaltic wave. Deglutitive inhibition is the phenomenon that allows animals

Table 5 Feeding requirements of fin whales engulfing 71 m^3 per lunge to fill forestomach (754 L) and meet metabolic demands (901 kg krill/day) at varying krill densities

Krill density (kg/m^3)	34.8[a]	4.5[b]	1.65[b]	0.5[b]	0.15[c]	0.05[d]	0.01[d]	0.003[d]
Krill per lunge (L)	2410.5	311.7	114.3	34.6	10.4	3.5	0.69	0.21
Water per lunge (L)	241.1	31.2	11.4	3.5	1	0.35	0.07	0.02
Krill + water (L)	2651.6	342.9	125.7	38.1	11.4	3.8	0.76	0.23
Times esophagus capacity	132.6	17.1	6.3	1.9	0.57	0.19	0.04	0.01
Lunges to fill FS	0.3	2.2	6.0	19.8	66	197.9	989.6	3298.5
Dives to fill FS	0.1	0.5	1.5	4.9	16.5	49.5	247.4	824.6
Time to fill FS (hrs)	0.01	0.1	0.2	0.7	2.5	7.4	37.1	123.7
Lunges to meet MD	0.4	2.8	7.7	25.4	84.6	253.8	1269	4230
Dives to meet MD	0.09	0.7	1.9	6.3	21.2	63.5	317.3	1057.5
Time to meet MD (hrs)	0.009	0.1	0.3	1.0	3.2	9.5	47.6	158.6

FS, forestomach; MD, metabolic demand.
[a](Nicol, 1987 (Nicol et al. 1987)).
[b](Goldbogen et al., 2011 (Goldbogen et al. 2011)).
[c](Croll et al., 2005 (Croll et al. 2005)).
[d](Goldbogen et al., 2015 (Goldbogen et al. 2015)).

Table 6 Feeding requirements of fin whales engulfing 30 m^3 per lunge to fill forestomach (754 L) and meet metabolic demands (901 kg krill/day) at varying krill densities

Krill density (kg/m^3)	34.8[a]	4.5[b]	1.65[b]	0.5[b]	0.15[c]	0.05[d]	0.01[d]	0.003[d]
Krill per lunge (L)	1018.5	131.7	48.3	14.6	4.4	1.5	0.29	0.09
Water per lunge (L)	101.9	13.2	4.8	1.5	0.44	0.15	0.03	0.01
Krill + water (L)	1120.4	144.9	53.1	16.1	4.8	1.6	0.32	0.1
Times esophagus capacity	56	7.2	2.7	0.81	0.24	0.08	0.02	0.005
Lunges to fill FS	0.7	5.2	14.2	46.8	156.1	468.4	2342	7806.6
Dives to fill FS	0.2	1.3	3.5	11.7	39.0	117.1	585.5	1951.6
Time to fill FS (hrs)	0.02	0.2	0.5	1.8	5.9	17.6	87.8	292.7
Lunges to meet MD	0.9	6.7	18.2	60.1	200.2	600.7	3003.3	10011.1
Dives to meet MD	0.2	1.7	4.6	15.0	50.1	150.2	750.8	2502.8
Time to meet MD (hrs)	0.02	0.3	0.7	2.3	7.5	22.5	112.6	375.4

FS, forestomach; MD, metabolic demand.
[a](Nicol, 1987 (Nicol et al. 1987)).
[b](Goldbogen et al., 2011 (Goldbogen et al. 2011)).
[c](Croll et al., 2005 (Croll et al. 2005)).
[d](Goldbogen et al., 2015 (Goldbogen et al. 2015)).

to drink fluids by performing rapid successive swallows by inhibiting the esophagus from completing an entire peristaltic contraction until the last swallow in the series, thus delaying the refractory period (Mashimo and Goyal 2006; Shaker et al. 2013). Even if deglutitive inhibition played a role in swallowing, 19 s is about two-thirds of the average inter-lunge time in a fin whale (30 s), and filtering prior to swallowing appears to take up most of the inter-lunge interval in whales (Goldbogen et al. 2013). Thus, it seems highly unlikely that a fin whale could purge all the water from the oral cavity and then swallow multiple boluses in only 30 s. Peristalsis is not the only driving force in bolus transit, though; pressure differentials created in the digestive tract during swallowing can speed up the transit time of the bolus (Standring and Gray 2021).

We predict that swallowing in a fin whale may happen according to the following model (Fig. 10). The VGB and tongue retract during the filtration stage of inter-lunge and bring the floor of the mouth back into

its resting position, mechanically filling the oral cavity with the fatty tongue and increasing pressure in the mouth. As this happens, space in the mouth is diminished, and food is likely concentrated at the back of the oral cavity on the non-compressible tongue. To transfer food from the mouth to the oropharynx, the oral plug must first be displaced from its position occluding the oropharyngeal channel to push food into the pharynx (Gil et al. 2022). The oral plug and soft palate are elevated dorsocaudally to block the nasopharynx and protect the upper airways from food incursion and clear the oropharyngeal channel. Opening the previously collapsed oropharynx by shifting the oral plug results in lower pressure in the oropharynx compared with the mouth. The tongue retracting fully into the mouth and the pressure differential between mouth and oropharynx forces the food through the oropharyngeal channel into the oropharynx, a zone of lower pressure. The tongue filling the oral cavity in its resting position provides a barrier between oral cavity and oropharynx. The protective configuration of pharyngeal structures during swallowing—with the soft palate and oral plug occluding the upper airways, and the closed and anteroventrally tucked larynx and laryngeal sac occluding the lower airways—would inhibit food from entering the respiratory tract (Gil et al. 2022). The muscular oropharynx can act as a pump that transports a slurry of food through the esophagus, like viscous fluid flow through a pipe, with a peristaltic wave at the end, as in deglutitive inhibition, to completely clear the esophagus. The thick skeletal muscle and connective tissues at the anterior end of the esophagus reinforce the esophageal wall to resist any damaging expansion under the pressure produced by the pharyngeal muscle.

The next feeding limitation is the capacity of the forestomach which, for a fin whale, averages ~750 L (Víkingsson 1997). Previous studies on feeding behavior have not considered this factor in whales (Goldbogen et al. 2019; Savoca et al. 2021), which will become important at high feeding rates. Based on the krill densities and fin whale feeding kinematics, we can estimate how many lunges and dives can take place before the forestomach is filled (Tables 5, 6). Fin whales average four lunges per dive, with dive duration and surface recovery time lasting 9 min (Goldbogen et al. 2007). This allows an estimate of the time it would take to fill the forestomach, or, the longest feeding bout a fin whale can engage in before it is full. When compared with observations of fin whale feeding bouts, the data match incredibly well. A study on the feeding habits of five fin whales found on average they performed 19 foraging dives lasting 2.7 h (Irvine et al. 2019). Our calculations suggest at a krill density of 0.15 kg/m^3 that a fin whale would fill its forestomach after 16.5 dives, in a total of 2.5 h.

There are multiple sources of variation that can explain the difference between observed and calculated feeding times—the actual volume of engulfment, varying krill densities across lunges, the time it takes swallowed water to pass through the forestomach compared to krill, or how much water is being consumed with krill. With all these variables the calculated value is impressively close to the observed, suggesting that forestomach capacity limits foraging bout duration. The digestion process in rorquals has not been investigated in detail but Víkingsson (Víkingsson 1997), in a study on stomach and digestive tract contents from commercially harvested fin whales, suggested a food transit time of 3–6 h from forestomach to fundic chamber, so feeding again within 3 h of a feeding bout is likely somewhat limited. Filling the forestomach once does not entirely meet predicted metabolic demands, so multiple feeding bouts must occur, particularly if seasonal metabolic demands are higher than the annual average. A 20 m long fin whale requires ~ 901 kg of krill per day to meet metabolic demands (Croll et al. 2006). Based on krill densities, the time it takes to meet metabolic demands can be calculated in the same manner (Tables 5, 6). This aspect of the model has been investigated previously (Goldbogen et al. 2007), but without considering stomach capacity or varying krill densities, both of which would impact the length of an actual feeding bout. From these data, we can see how many more foraging dives are required to meet metabolic demands once food processing in the stomach has started. In a recent modeling study, Savoca et al. (2021) suggested that during a 90–120 day summer feeding season a fin whale may make 200–300 lunges (50–75 dives) and consume 5000–10,000 kg of krill per day. That figure is up to an order of magnitude higher than both the forestomach capacity and metabolic demands measured and calculated, respectively, of a fin whale. While this engulfment rate is plausible, it is difficult to understand how these whales could process such large volumes of food that quickly.

Feeding style and prey type between rorquals and odontocetes are vastly different, and the anatomy of the esophagus reflects this. In the fin whale, esophagus morphology is unusual, with a small lumen, high collagen content in the first two-thirds of the esophagus, incredibly high adipose content in the last one-third, and the presence of a third muscle layer that is likely part of the submucosa. Histology from normal human esophagi (Young et al. 2014; Pawlina and Ross 2016) shows far less adipose content compared to the fin whale. Likewise, the odontocete esophagus showed no adipose tissue along its length. The muscularis propria cannot be

stretched very much—perhaps this adipose layer enables an increase in lumen size for bolus transport to occur without stretching the muscularis propria. The muscularis mucosae muscle layer in fin whales could provide an increased ability to tonically resist damaging expansion forces, as well as assist with increasing force production or speed for the final peristaltic wave to clear the esophagus. Additionally, the fin whale esophagus has striated muscle quite far posteriorly, likely meaning a rapid rate of peristalsis. Unfortunately, we are unaware at what point the transition to smooth muscle occurs in odontocetes. We assume that the fin whale has striated muscle further posteriorly to decrease food transport time for the time-limited feeding events of fin whales.

Rorquals may be the only mammals, and possibly the only animals, that capture a volume of food that is too large to be swallowed as a single distinct bolus without processing in the oral cavity. This requires an ability to transport large volumes of food to the stomach while on a time-limited dive; thus, performing these tasks rapidly is energetically advantageous. The rorqual esophagus should be adapted to meet transport requirements, and the morphology and mechanics revealed in this study support that. The fin whale esophagus has a small luminal width surrounded by thick muscular walls, capable of expanding around a fluid-like bolus and generating and withstanding forceful peristaltic pressures. The volume of food a fin whale engulfs is dictated by krill densities in nature, while the timing of lunging is dictated by the morphology and mechanics of the esophagus. Rorquals are incredibly successful at feeding considering that they include the largest animals on the planet. Their adaptations for engulfing immense volumes of prey are largely credited for their large body size; however, adaptations of the digestive tract are also imperative to their success and should not be overlooked.

Acknowledgments

The authors thank Kristján Loftsson and the staff at Hvalur hf, Iceland, and Daníel Halldórsson at the Marine and Freshwater Research Institute, Reykjavík, Iceland. We thank Gísli Víkingsson for his studies on the fin whale stomach, supporting our research endeavour and providing valuable resources to us, Stephen Raverty for helping obtain permits, and Margo Lillie for help dissecting and performing mechanical tests on specimens, and for valuable biomechanics discussions. Hannes Petersen provided the Icelandic translation. Cover photo courtesy of the Duke Marine Robotics & Remote Sensing Lab under NMFS Permit 16111.

Funding

This work was supported by Natural Sciences and Engineering Research Council of Canada Discovery Grant RGPIN-10 2019-04235 (R.E.S.); Natural Sciences and Engineering Research Council of Canada Discovery Grant RGPIN-12 2018-03727 (A.W.V.).

Competing Interests

The authors declare no competing interests.

References

Arnold PW, Birtles RA, Sobtzick S, Matthews M, Dunstan A. 2005. Gulping behaviour in rorqual whales: underwater observations and functional interpretation. Mem Queensl Mus 51:309–32.

Brodie PF. 1993. Noise generated by the jaw actions of feeding fin whales. Can J Zool 71:2546–50.

Croll DA, Kudela R, Tershy BR. 2006. Ecosystem impact of the decline of large whales in the North Pacific. In Whales, Whaling and Ocean Ecosystems (ed. J.A. Estes), Berkeley, CA: University of California Press. p. 202–14.

Croll DA, Marinovic B, Benson S, Chavez FP, Black N, Ternullo R, Tershy BR. 2005. From wind to whales: trophic links in a coastal upwelling system. Mar Ecol Prog Ser 289:117–30.

Gil KN, Vogl AW, Shadwick RE. 2022. Anatomical mechanism for protecting the airway in the largest animals on earth. Curr Biol 32:1–6.

Gil KN, Vogl AW, Shadwick RE. 2022. Anatomical mechanism for protecting the airway in the largest animals on earth. Curr Biol 32:898–903.e1.

Goldbogen J, Pyenson N, Shadwick R. 2007. Big gulps require high drag for fin whale lunge feeding. Mar Ecol Prog Ser 349:289–301.

Goldbogen JA, Cade DE, Wisniewska DM, Potvin J, Segre PS, Savoca MS, Hazen EL, Czapanskiy MF, Kahane-Rapport SR, DeRuiter SL et al. 2019. Why whales are big but not bigger: physiological drivers and ecological limits in the age of ocean giants. Science 366: 1367–72.

Goldbogen JA, Calambokidis J, Oleson E, Potvin J, Pyenson ND, Schorr G, Shadwick RE. 2011. Mechanics, hydrodynamics and energetics of blue whale lunge feeding: efficiency dependence on krill density. J Exp Biol 214:698–9.

Goldbogen JA, Calambokidis J, Shadwick RE, Oleson EM, McDonald MA, Hildebrand JA. 2006. Kinematics of foraging dives and lunge-feeding in fin whales. J Exp Biol 209:1231–44.

Goldbogen JA, Friedlaender AS, Calambokidis J, McKenna MF, Simon M, Nowacek DP. 2013. Integrative approaches to the study of Baleen whale diving behavior, feeding performance, and foraging ecology. Bioscience 63:90–100.

Goldbogen JA, Hazen EL, Friedlaender AS, Calambokidis J, DeRuiter SL, Stimpert AK, Southall BL. 2015. Prey density and distribution drive the three-dimensional foraging strategies of the largest filter feeder. Funct Ecol 29:951–61.

Goldbogen JA, Madsen PT. 2018. The evolution of foraging capacity and gigantism in cetaceans. J Exp Biol 221:jeb166033.

Goldbogen JA, Potvin J, Shadwick RE. 2010. Skull and buccal cavity allometry increase mass-specific engulfment capacity in fin whales. Proc R Soc B Biol Sci 277:861–8.

Gregersen H. 2003. Biomechanics of the Gastrointestinal Tract: New Perspectives in Motility Research and Diagnostics. Springer Science & Business Media.
Harrison RJ, Johnson FR, Young BA. 1970. The oesophagus and stomach of dolphins (Tursiops, Delphinus, Stenella). J Zool 160:377–90.
Hazen EL, Friedlaender AS, Goldbogen JA. 2015. Blue whales (*Balaenoptera musculus*) optimize foraging efficiency by balancing oxygen use and energy gain as a function of prey density. Sci Adv 1:e1500469.
Irvine LM, Palacios DM, Lagerquist BA, Mate BR. 2019. Scales of blue and fin whale feeding behavior off California, USA, with implications for prey patchiness. Front Ecol Evol 7:338.
Lillie MA, Chalmers GWG, Gosline JM. 1994. The effects of heating on the mechanical properties of arterial elastin. Connect Tissue Res 31:23–35.
Lillie MA, Piscitelli MA, Vogl AW, Gosline JM, Shadwick RE. 2013. Cardiovascular design in fin whales: high-stiffness arteries protect against adverse pressure gradients at depth. J Exp Biol 216:2548–63.
Mashimo H, Goyal R. 2006. Physiology of esophageal motility. In: GI Motility Online. PART 1 Oral Cavity, Pharynx and Esophagus. Heidelberg: Springer Nature. https://www.nature.com/gimo/contents/pt1/full/gimo3.html.
Mittal RK, Padda B, Bhalla V, Bhargava V, Liu J. 2006. Synchrony between circular and longitudinal muscle contractions during peristalsis in normal subjects. Am J Physiology-Gastrointestinal Liver Physiol 290: G431–8.
Nicol S, James A, Pitcher G. 1987. A first record of daytime surface swarming by euphausiaiucens in the Southern Benguela region. Mar Biol 94:7–10.
Oezcelik A, DeMeester SR. 2011. General anatomy of the Esophagus. Thorac Surg Clin 21:289–97.
Pawlina W, Ross MH. 2016. Digestive System II: esophagus and gastrointestinal tract. In Histology; a Text and Atlas with Correlated Cell and Molecular Biology. Wolters Kluwer Health, Inc., p. 568–625.
Pehlivanov N, Liu J, Kassab GS, Puckett JL, Mittal RK. 2001. Relationship between esophageal muscle thickness and intraluminal pressure: an ultrasonographic study. Am J Physiology-Gastrointestinal and Liver Physiol 280:G1093–8.
Potvin J, Goldbogen JA, Shadwick RE. 2009. Passive versus active engulfment: verdict from trajectory simulations of lunge-feeding fin whales *balaenoptera physalus*. J R Soc Interface 6: 1005–25.
Puckett JL, Bhalla V, Liu J, Kassab G, Mittal RK. 2005. Oesophageal wall stress and muscle hypertrophy in high amplitude oesophageal contractions. Neurogastroenterol Motil 17: 791–9.
Rospars J-P, Meyer-Vernet N. 2016. Force per cross-sectional area from molecules to muscles: a general property of biological motors. R Soc Open Sci 3:160313.
Savoca MS, Czapanskiy MF, Kahane-Rapport SR, Gough WT, Fahlbusch JA, Bierlich KC, Segre PS, Di Clemente J, Penry GS, Wiley DN et al. 2021. Baleen whale prey consumption based on high-resolution foraging measurements. Nature 599:85–90.
Scales H, Smith C. 2010. Could a human survive swallowing by a whale? The Naked Scientists. https://www.thenakedscientists.com/articles/questions/could-human-survive-swallowing-whale. Accessed on June 27, 2010.
Schindelin J, Arganda-Carreras I, Frise E, Kaynig V, Longair M, Pietzsch T, Preibisch S, Rueden C, Saalfeld S, Schmid B et al. 2012. Fiji: an open-source platform for biological-image analysis. Nat Methods 9:676–82.
Shaker R., Belafsky P.C., Postma G.N., Easterling C. eds. 2013. Principles of Deglutition. Springer: New York, NY.
Standring S, Gray H. 2021. Gray's Anatomy: the Anatomical Basis of Clinical Practice. 42nd ed. Elsevier Limited.
Sukon P. 2002. The physiology and anatomy of the esophagus of normal llamas and llamas with megaesophagus. Oregon State University ProQuest Dissertations & Theses, 2002. 3056578.
Tarpley RJ. 1985. Gross and microscopic anatomy of the tongue and gastrointestinal tract of the Bowhead Whales (*Balaena mysticetus*). Texas A&M University ProQuest Dissertations & Theses, 1985. 8605226.
Víkingsson GA. 1997. Feeding of fin whales (*Balaenoptera physalus*) off Iceland–diurnal and seasonal variation and possible rates. J Northw Atl Fish Sci 22:77–89.
Yamasaki F, Takahashi K. 1971. Digestive tract of Ganges dolphin, *Platanista gangetica*. Okajimas Folia Anat Jpn 48:271–93.
Young B, O'Dowd G, Woodford P. 2014. Wheater's Functional Histology; a Text and Colour Atlas 6th ed. Elsevier Churchill Livingstone.
Young B, O'Dowd G, Woodford P. 2014. Gastrointestinal tract. In: Wheater's Functional Histology; a Text and Colour Atlas. Elsevier Churchill Livingstone. p. 251–75.